Infectious Disease Modelling 7 (2022) 64–74

Contents lists available at ScienceDirect

Infectious Disease Modelling

journal homepage: www.keaipublishing.com/idm

First-wave COVID-19 daily cases obey gamma law

Jean Duchesne [a], Olivier A. Coubard [b, *]

[a] Agrocampus Ouest, 2 rue André Le Nôtre, 49000, Angers, France
[b] The Neuropsychological Laboratory, CNS-Fed, 240 rue de Rivoli, 75001, Paris, France

ARTICLE INFO

Article history:
Received 12 September 2021
Received in revised form 29 January 2022
Accepted 27 February 2022
Available online 11 March 2022
Handling Editor: Dr HE DAIHAI HE

Keywords:
COVID-19
Epidemiology
Gamma law
Humans
Statistical physics

ABSTRACT

Modelling how a pandemic is spreading over time is a challenging issue. The new coronavirus disease called COVID-19 does not escape this rule as it has embraced over two hundred countries. As for previous pandemics, several studies have attempted to model the occurrence of cases caused by COVID-19. However, no study has succeeded in accurately modelling the impact of the infectious agent. Here we show that COVID-19 daily case distribution in humans obeys a Gamma law, which two new parameters can describe without any adjustment. Though the Gamma law has been exploited for nearly two centuries to describe the statistical distribution of spatial or temporal quantities, the goodness-of-fit rationale using two or three parameters has remained enigmatic. The new Gamma law approach we demonstrate here emerges from actual data and sheds light on the underlying mechanisms of the observed phenomenon. This finding has promising applicability in the epidemiological domain and in all disciplines involving branching systems, for which our Gamma law approach may bring a solution to hitherto unsolved problems.

1. Introduction

Since 2019, the coronavirus disease so-called COVID-19 caused by the infectious agent SARS-CoV-2 has contaminated more than three hundred million humans worldwide and killed more than five million of them. Modelling the spread of an infectious disease in general and, in particular, a viral disease is challenging to achieve. According to Neuberger et al. (Neuberger, Paul, Nizar, & Raoult, 2013), appropriate modelling oscillates between haphazard and hazard. The contamination dynamics of an infectious agent are typically studied using the mathematics of variable complexity. At the same time, the objective of model formulation and analysis may take roots in many different frameworks (Anderson & May 1991). Conceptual models are based on equations set a priori and parameters adjusted a posteriori, whether they apply to viruses in general (Graw & Perelson, 2016) or the specific case of COVID-19 (Lin et al., 2020). A variety of models have been proposed to date to analyze or predict the evolution of an epidemic. For instance, the Susceptible-Exposed-Infectious-Removed (SEIR) model has been widely used (Lin et al., 2020; Sanche et al., 2020). The Global Epidemic and Mobility (GLEAM) project proposes stochastic models of disease transmission based on real-world data on populations and human mobility to promote intervention strategies that minimize the impact of epidemics (Chinazzi et al., 2020). Using this framework, Balcan et al.

* Corresponding author. Tel.: +331 45 493608.
E-mail addresses: jean.duchesne@live.fr (J. Duchesne), olivier.coubard@cns-fed.fr (O.A. Coubard).
Peer review under responsibility of KeAi Communications Co., Ltd.

https://doi.org/10.1016/j.idm.2022.02.004

(Balcan et al., 2009) have decomposed the earth's surface into Voronoi cells, which were centered on international airports, and shown multiscale mobility networks in the spreading of diseases.

Here we introduce a new approach based on statistical physics whose goal is to provide a general and robust model of the evolution over time of a natural phenomenon. Our approach is based on available data without any adjustment before or after the mathematics. Let us first consider that the COVID-19 virus spread describes a tree as follows (Cauchemez et al., 2011; Faye et al., 2015). In a first cascade, the first infected individual (patient P_0) contaminated on average R patients P_1. The ratio or reproductive number R is usually noted R_0 at the beginning of the epidemic. This has well been defined by Anderson et al. (Anderson et al., 2004), studied by Zhang et al. (Zhang et al., 2020) for the *Diamond Princess* cruise ship, and discussed by Thomson et al. (Thompson et al., 2020). In a second cascade, the R patients P_1 contaminate R^2 patients P_2, and so on. This way, we get a propagation tree with n cascades. Fig. 1 shows a simplified contamination tree. The line segment P_0E_0 represents the contagiousness duration of patient P_0, where points P_0/ E_0 are the beginning/end, respectively. After time l_1 (line segment P_0P_1), the patient P_0 contaminates a first patient P_1. Then, after another value of l_1 (line segment $P_0P'_1$), a second patient P_1 is contaminated and so on. In Fig. 1, the longest contamination chain has the length L defined as in Equation (1).

$$L = l_1 + l_2 + l_3 \tag{1}$$

where $l_1 = P_0P'_1$; $l_2 = P'_1P'_2$; $l_3 = P'_2P''_3$.

If the time taken by a patient P_i to contaminate the R^{i+1} patients P_{i+1} was always the same, and if R was constant, it would be easy to fix the number of cases at every moment of the epidemic corresponding to every end of n cascades. This is unfortunately not the case. Thus, we note l_i the length of the i^{th} cascade as the time taken by a patient P_{i-1} to contaminate one of the R patients P_i, which time scale may vary (days, hours, etc.). Let us keep in mind that l_i does not have the same value for all contaminated patients P_i. Consequently, the length of the contamination chain, which is the time between P_0 contamination and that of any of the patients P_n in the n^{th} cascade, can be expressed as the total length L of n components l_i as in Equation (2).

$$L = \sum_{i=1}^{n} l_i \tag{2}$$

The l_i components are the times spent in steps $1, 2, \ldots, i, \ldots n$ of the contamination chain. This time l_i has been elsewhere called serial interval by Zhang et al. (Zhang et al., 2020). In the Supplementary Material S1 section, we demonstrate that the probability density function (PDF) of the variable L can be expressed by a Gamma law as in Equation (3).

$$F(L) = \frac{1}{(2\bar{l})^{\frac{n}{2}}} \frac{1}{\Gamma\left(\frac{n}{2}\right)} L^{\left(\frac{n}{2}-1\right)} e^{-\frac{L}{2\bar{l}}} \tag{3}$$

In Equation (3), $\bar{l}$ is the average length of components l_i; Γ is the Gamma function of Euler; L is the length of the contamination chain between patient P_0 and any of the contaminated patients; n is the number of cascades required to pass

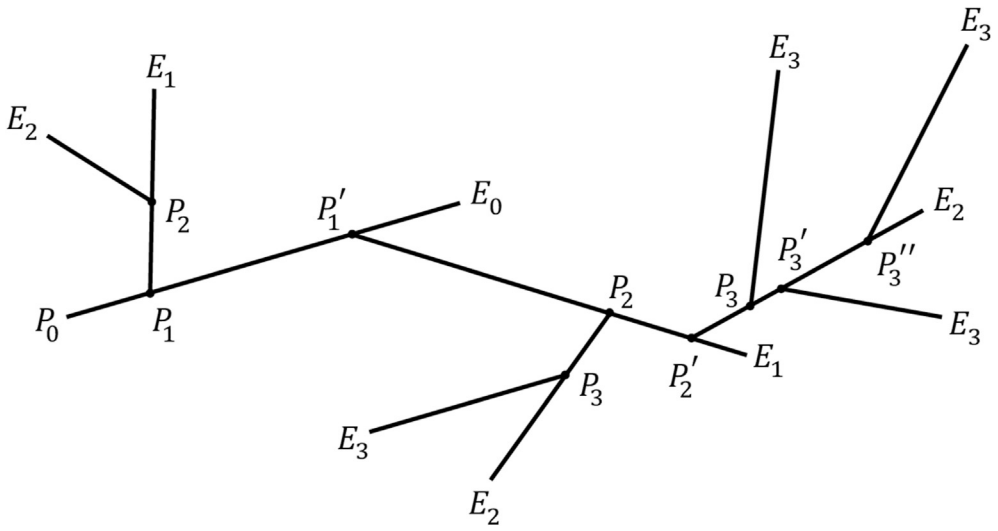

Fig. 1. Schema of COVID-19 contamination tree. Points *P*/*E* represent the start/end, respectively, of the contagiousness duration of patient P_0, patient P_1 and so on.

from the patient P_0 to any of the patients P_n; m is the average of contamination chain length with $m = \bar{L}$. Therefore, we get $\bar{l} = \frac{\bar{L}}{n}$. Two new parameters, the number of cascades n and the average length of the contamination chain component $\bar{l}$, add value to the traditional ones, the shape parameter α and the scale parameter β of the Gamma law (Woo, 1999) of Equation (4).

$$F(L) = \left(\frac{1}{\beta}\right)^{\alpha} \frac{1}{\Gamma(\alpha)} L^{\alpha-1} e^{-\frac{L}{\beta}} \tag{4}$$

According to Lancaster (Lancaster, 1966), we owe the Gamma law to Laplace (Laplace, 1836). For 186 years, the Gamma law has used two (sometimes three) parameters, α and β, to model a phenomenon over time, which are not obviously meaningful even for the experts of the field. Here, we propose that our new parameters n and $\bar{l}$ are likely to shed light on the underlying mechanisms of the studied phenomenon. In epidemiology, n and $\bar{l}$ can be meaningful by representing the number of branches or cascades and the average length of a branch or cascade, respectively.

This article used our new Gamma law approach to elucidate how COVID-19 first-wave has spread in different countries. In three studies, we show that this approach best fits the pandemic's natural course over time compared to other distributions.

2. Results

We develop the Methods in the Supplementary Material S2 section and show the results in Tables 1 and 2 and Figs. 2–4.

2.1. Study 1: entering the COVID-19 pandemic

In a first study, we examined COVID-19 case distribution in five countries: China, Germany, Austria, Israel, and New Zealand (see Table 1 lines 1–5 and Fig. 2).

We first selected China, where the epidemic presumably started in Wuhan, Hubei province. Let us decline the variables in Table 1, line 1. The rate of cases per mille residents for the whole country was 0.05‰. The first-wave epidemic lasted 54 days and concerned 77,251 cases between January 22 and March 16, 2020. According to our Gamma approach (see Introduction section), the number n of individuals between the zero case and any case was 17, and the average duration of contamination $\bar{l}$ between one individual and another was 1.3 days (see Table 1 line 1).

We plotted the same data in Fig. 2A, showing the histogram of probability density function (PDF) in frequency as a function of time in days. As one may observe, two raw aberrant values of 14,108 and 5090 cases on February 12th and 13th led to seven aberrant values in the 7-day moving average. These values rather than insincere might be inherent in the difficulty to count cases (and the necessity to catch up) in the early stage of the epidemic. Other countries have also exhibited in their count of cases catching-up values. For that reason, we decided to let the data as they are rather than correcting them. We plotted observed data against our Gamma approach and the Lognormal law as a control since the two laws have previously been used in concurrence (e.g., Cho, Bowman, & North, 2004). Notably, the Kolmogorov-Smirnov was calculated on the cumulative density functions (CDF) so that the P-value on the CDF may sometimes unfit the reader's visual impression of the PDF. Due to aberrant values, theoretical fits are not as good as expected. However, considering the higher the P-value the better the

Table 1
For the COVID-19 first-wave in 2020 and for each country (CH, China; GE, Germany; AU, Austria; IS, Israel; NZ, New Zealand; BE, Belgium; SP, Spain; IT, Italy; FR, France; FI, Finland; CZ, Czechia; SL, Slovenia; LI, Lithuania; CR, Croatia; LA, Latvia), we report the rate of cases per mille residents (Case/pop), numbers of days, total number of cases, mean (in days) and variance σ^2 of the observed distribution of daily cases; n (number) and $\bar{l}$ (in days) values of the Gamma distribution; peak values (in frequency) of the observed and Gamma distributions; and P values of the Kolmogorov-Smirnov test between the observed distribution and, respectively, Gamma (P1) and Lognormal (P2) distributions.

Country	Case/Pop	Days	Cases	Mean	σ^2	n	$\bar{l}$	Peak^{ob}	Peak^{ga}	P1	P2
Study 1											
CH	0.05‰	54	77,251	21.6	56.2	17	1.3	0.060	0.056	0.735	0.572
GE	2.24‰	119	186,639	56.7	346.0	19	3.1	0.031	0.022	0.984	0.460
AU	1.76‰	72	15,701	35.0	125.4	20	1.8	0.048	0.037	0.874	0.607
IS	1.76‰	96	16,620	54.8	158.1	38	1.4	0.037	0.032	0.042	0.018
NZ	0.29‰	75	1497	32.5	84.7	25	1.3	0.050	0.045	0.497	0.275
Study 2											
BE	5.33‰	122	61,272	50.4	445.8	11	4.4	0.024	0.020	0.986	0.951
SP	4.94‰	85	234,188	42.9	184.3	20	2.1	0.037	0.031	0.710	0.347
IT	3.98‰	132	240,325	51.0	496.8	10	4.9	0.024	0.020	0.991	0.832
FR	2.00‰	100	135,114	54.8	254.3	24	2.3	0.031	0.026	0.683	0.266
FI	1.31‰	133	7256	56.9	543.1	12	4.8	0.023	0.018	0.992	0.215
CZ	0.76‰	72	8160	37.3	188.8	15	2.5	0.032	0.031	0.959	0.749
SL	0.70‰	81	1467	29.3	197.8	9	3.4	0.033	0.032	0.681	0.020
LI	0.58‰	81	1619	32.5	337.9	6	5.2	0.033	0.025	0.976	0.681
CR	0.56‰	77	2193	41.8	174.2	20	2.1	0.034	0.032	0.393	0.290
LA	0.56‰	89	1072	37.9	410.4	7	5.4	0.030	0.023	0.853	0.282

Table 2
For the COVID-19 first-wave in 2020 and for each country (CH, China; GE, Germany; AU, Austria; IS, Israel; NZ, New Zealand; BE, Belgium; SP, Spain; IT, Italy; FR, France; FI, Finland; CZ, Czechia; SL, Slovenia; LI, Lithuania; CR, Croatia; LA, Latvia), we report the P values of the Kolmogorov-Smirnov test between the observed distribution and, respectively, Gamma (P1), Gaussian (P3) and Weibull (P4) distributions. The Lognormal distribution (P2) is not shown (see Table 1). Gray cells show the superiority of other than Gamma distributions.

Country	Gamma P1	Gaussian P3	Weibull P4
Study 1			
CH	0.735	0.572	0.735
GE	0.984	0.063	0.367
AU	0.874	0.874	0.959
IS	0.042	0.955	0.090
NZ	0.497	0.196	0.771
Study 2			
BE	0.986	0.176	0.034
SP	0.710	0.833	0.833
IT	0.991	0.121	0.007
FR	0.683	0.266	0.563
FI	0.992	0.351	0.165
CZ	0.959	0.607	1.000
SL	0.681	0.914	0.077
LI	0.976	0.681	0.020
CR	0.393	0.969	0.898
LA	0.853	0.610	0.103

goodness of fit (Massey Jr., 2012), the Gamma curve led to a higher value than the Lognormal one. It also predicted a peak in the curve only three days earlier than observed.

In the first group, we added four countries where the public health policy has been strict in detecting and isolating cases, at least in the early stage of the pandemic: Germany (Laffet, Haboubi, Elkadri, Georges Nohra, & Rothan-Tondeur, 2021), Austria (Moshammer, Poteser, Lemmerer, Wallner, & Hutter, 2020), Israel (Yom-Tov, 2021), and New Zealand (Bandyopadhyay & Meltzer, 2020). We show the data in Table 1, lines 2–5 and Fig. 2B, where we sorted the countries by decreasing impact defined as the rate of cases per mille residents (reverse range = 2.24‰–0.29‰).

Taken together with China, the parameter n was 24 ± 9 (range = 17–38), and the parameter $\bar{l}$ was 1.8 ± 0.7 days (range = 1.3–3.1 days).

Fig. 2B shows that, again, the Gamma distribution better fitted the Lognormal one as evidenced by a higher P-value for the four countries, should the observed curve be either smooth (Germany and Austria) or noisy (Israel and New Zealand). One may also see the precision of our Gamma approach in calculating the date of the peak value in case frequency: four days later between the theoretical and observed distributions for Germany, one day later for Austria, two days later for Israel, and two days earlier for New Zealand (see Fig. 2B).

Then, we observed the results in countries with a different public health policy, as the pandemic can end when the availability of susceptible individuals or the reproductive rate decreases (Cobey, 2020).

2.2. Study 2: Top ten most impacted countries by first-wave COVID-19 pandemic

In a second study, we examined COVID-19 case distribution in ten countries where the public health policy has been less strict than the ones above: Belgium, Spain, Italy, France, Finland, Czechia, Slovenia, Lithuania, Croatia, and Latvia. We show the data in Table 1, lines 6–15 and Fig. 3, where we also sorted countries by decreasing impact (reverse range = 5.33‰–0.56‰).

For this second group of countries, the parameter n was 13 ± 6 (range = 6–24), and the parameter $\bar{l}$ was 3.7 ± 1.4 days (range = 2.1–5.4 days).

Fig. 3 shows that, again, the Gamma distribution offered a better fit than did the Lognormal distribution, as evidenced by a higher P-value for the ten countries, regardless of the shape of the observed curve. Again, our Gamma approach accurately

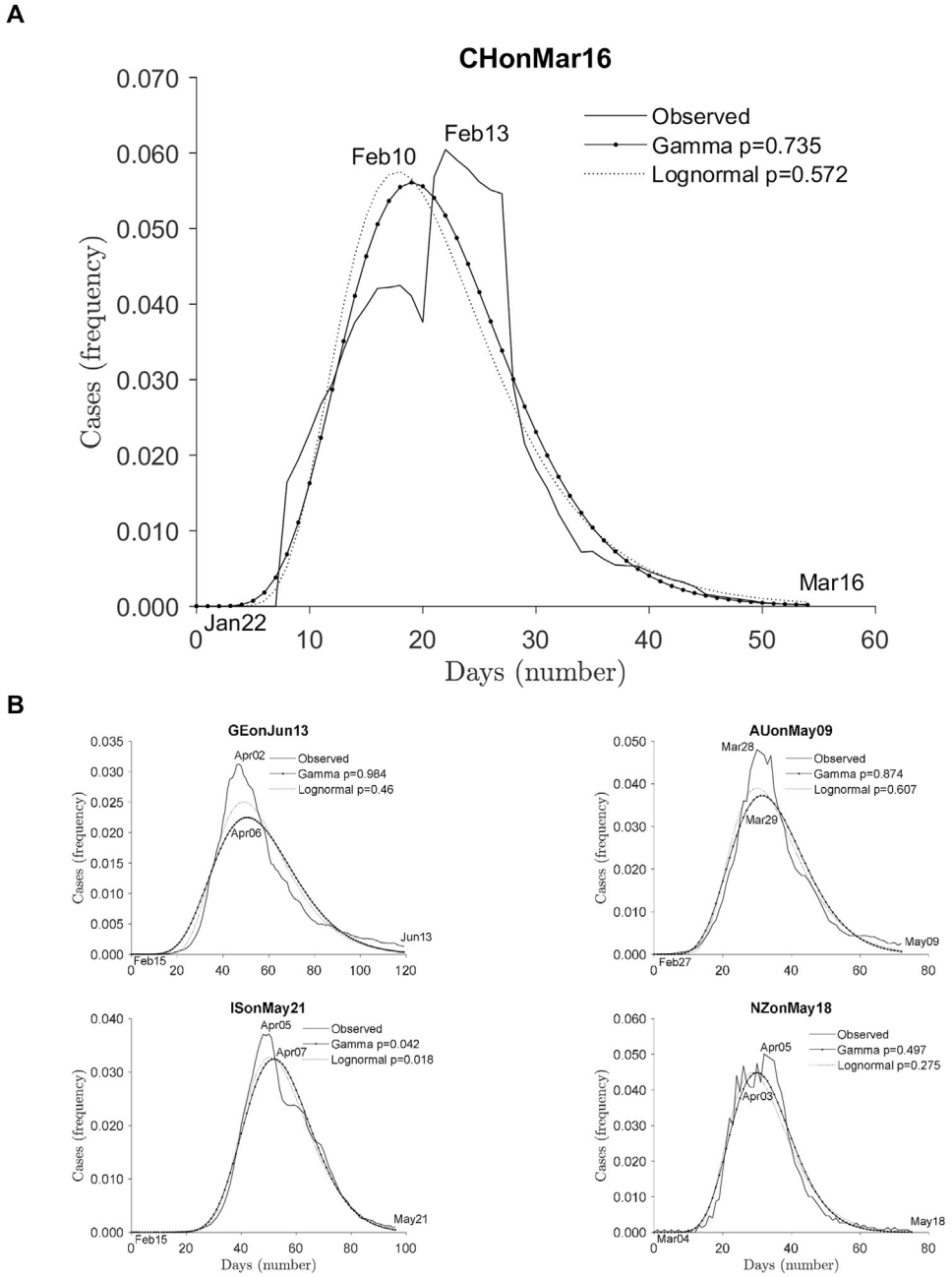

Fig. 2. Study 1. Histogram of probability density function (in frequency) of COVID-19 observed daily cases in (**A**) China (CH) and (**B**) Germany (GE), Austria (AU), Israel (IS), and New Zealand (NZ) using 7-day moving averages (solid line) and their theoretical fits by Gamma (solid-dotted line) and Lognormal (dotted line) distributions as a function of time (in days). P values are those of Kolmogorov-Smirnov tests between the observed distribution and each theoretical one. Tags indicate the corresponding dates of beginning, peaks of observed and Gamma distributions, and end in 2020.

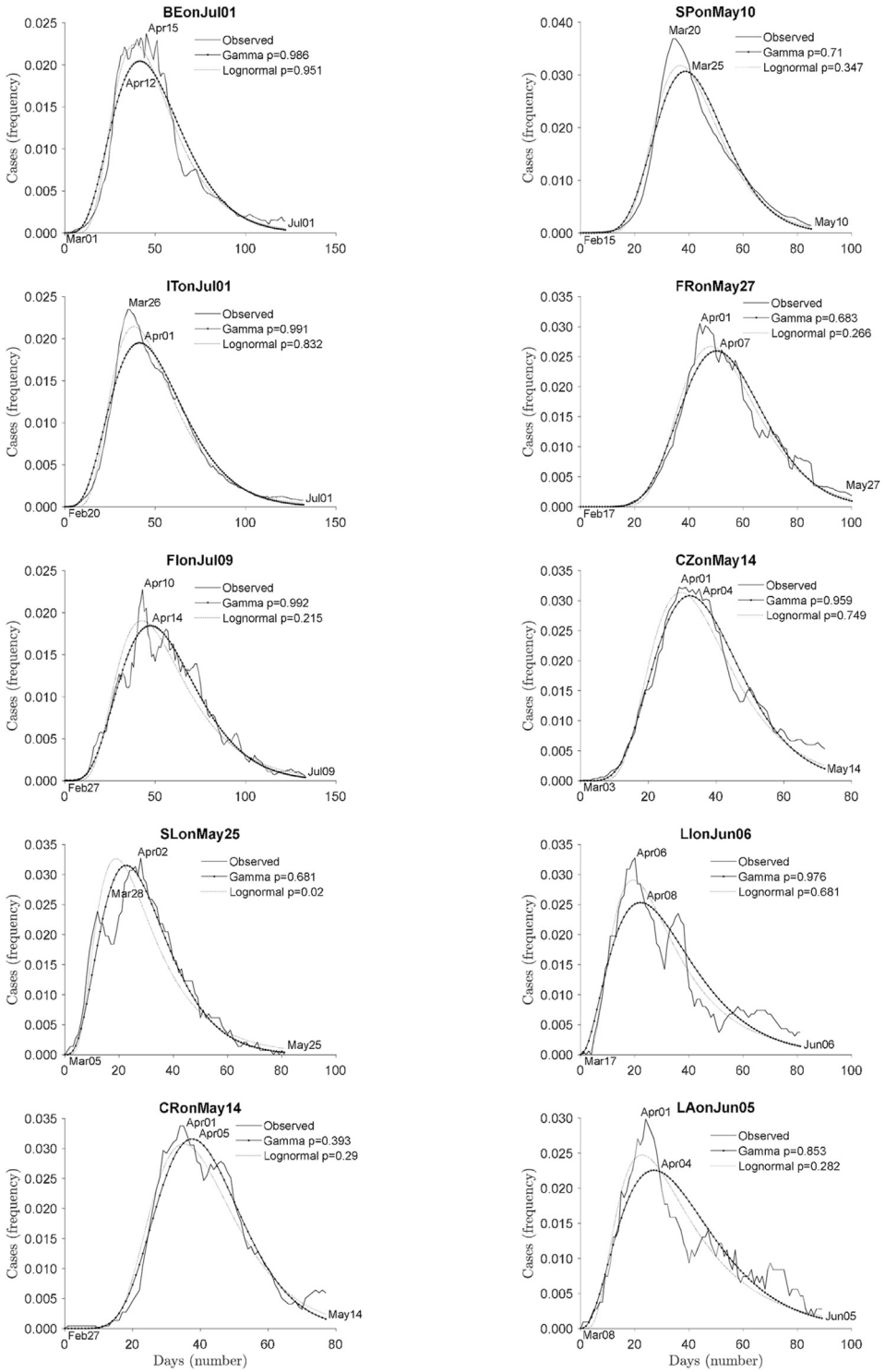

Fig. 3. Study 2. Histogram of probability density function (in frequency) of COVID-19 observed daily cases in Belgium (BE), Spain (SP), Italy (IT), France (FR), Finland (FI), Czechia (CZ), Slovenia (SL), Lithuania (LI), Croatia (CR), and Latvia (LA). Other notations as in Fig. 2.

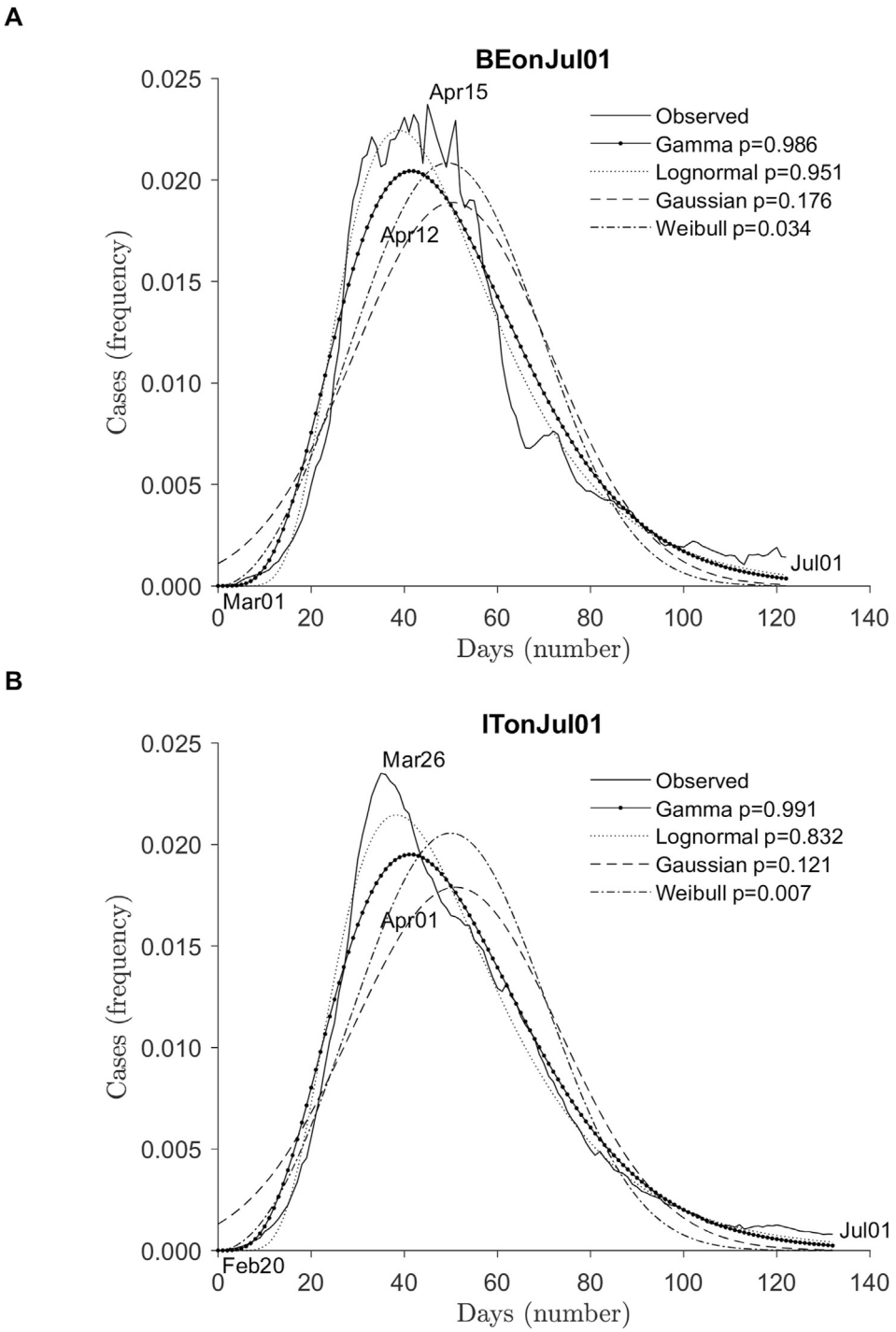

Fig. 4. Study 3. Histogram of probability density function (in frequency) of COVID-19 observed daily cases in Belgium (BE) and Italy (IT) using 7-day moving averages (solid line) and their theoretical fits by Gamma (solid-dotted line), Lognormal (dotted line), Gaussian (dashed line), and Weibull (dash-dotted line) distributions as a function of time (in days). Other notations as in Fig. 2.

calculated the peak value in daily case frequency: from a minimum difference between the observed distribution and the Gamma fit of two days for Lithuania to six days for France (see Fig. 3).

Finally, we compared the two groups of countries (Study 1 vs. Study 2). The between-group difference was different for parameter $\bar{l}$ (Mann-Whitney U test, $Z = -2.57$, $P < .05$), but not for parameter n due to high variability ($Z = 1.96$, $P > .05$).

2.3. Study 3: Fine-tuning the comparison between gamma and other distributions

As one may argue that the Lognormal distribution is insufficient to demonstrate our Gamma approach's superiority, we conducted another control using further distributions. While Poisson and Gumbel were excluded for theoretical reasons (see Discussion section), we challenged our Gamma approach with Gaussian and Weibull distributions.

Gaussian and Weibull distributions have frequently been used in medical studies (Collett, 2015). Furthermore, the Weibull distribution has recently been proposed to model the serial interval distribution in the COVID-19 pandemic (Adam et al., 2020). We can write the Weibull PDF as in Equation (5):

$$\frac{a}{b}\left(\frac{x}{b}\right)^{a-1} \tag{5}$$

where a and b are the shape and scale parameters, respectively.

The Weibull mean is $b\Gamma\left(1+\frac{1}{a}\right)$ where Γ is the Euler gamma function. We manually set the shape parameter a by trial and error, then b is calculated from a. In our study, we obtained the best result when a was set to 3 so that b was 55.

Data for the fifteen countries of studies 1 and 2 are shown in Table 2 and for two countries in Fig. 4.

As shown in Table 2, our Gamma distribution offered a better fit and corresponding P-value than did other distributions in most, but not all, cases. Indeed, whereas Gamma distribution better fitted the observed curve compared to Lognormal distribution in 100% of the fifteen countries (see Table 1), the Gamma distribution better fitted the empirical distribution in 11/15 or 73% of countries when compared to the Gaussian one, and in 9/15 or 60% of countries when confronted to the Weibull one.

For clarity of display, Fig. 4 shows only two countries that the early stage of the pandemic dramatically hit: Belgium and Italy. As evidenced by P-values, the Gamma distribution better fitted the observed data than all other distributions in these two examples.

3. Discussion

The present study introduced a new view of the well-known Gamma law, in which we now set the parameters from a statistical-physics-based calculation. Using data from fifteen countries undergoing the COVID-19 pandemic, we showed the goodness-of-fit of the Gamma law compared to other distributions. The main findings were as follows. (1) In fifteen countries where the public health policy has been either rigorous or accommodating, our Gamma law approach better fitted the distribution of observed daily cases of COVID-19 than did another skewed distribution, the Lognormal law, in 100% of countries. (2) Using symmetrical (Gaussian) or other skewed (Weibull) distributions, our Gamma law approach better fitted the observed data in 73% of countries against the Gaussian law and 60% of countries against the Weibull one. (3) New Gamma parameters, number n and mean component length $\bar{l}$, may help to understand further the underlying mechanisms of the observed phenomenon. After discussing methodological issues regarding the distributions, we comment on our results in the two groups of countries.

In our study, a critical issue was the choice of control distributions to challenge our Gamma law proposal. Many distributions have been used in medical studies, should they have a positive skewness as Gamma or not (Collett, 2015). We could not use the Poisson distribution as its unique parameter λ equals both the mean and the variance, which was not the case in our observed data. The Gumbel distribution exhibits a positive skewness, and its PDF is given by Equation (6):

$$\frac{\exp(-z)}{\beta} \tag{6}$$

where. $z = exp\left(-\frac{x-m}{\beta}\right)$

and where the m is the mean of variable x and β a given parameter.

Though the Gumbel distribution is easy to use as it involves only one parameter, we abandoned it as no value of β provided a satisfying result. The Lognormal distribution, another skewed distribution used elsewhere against Gamma distribution in meteorology or hydrology (Cho et al., 2004), was chosen as an excellent theoretical fit in our Study 1, though weaker than our Gamma approach. Study 3 introduced the Gaussian distribution as a possible control, and 4/15 countries showed that the observed data could fit a symmetrical distribution, consistent with previous studies (Adam, 2020; Ferguson et al., 2005; Ferguson et al., 2006). Ferguson et al. (Ferguson et al., 2006) modelled the mitigation of the influenza pandemic and ended up with a Gaussian distribution to describe the evolution of cases. Gaussian and Gamma plots can become similar when n reaches a high value of 80 or more. More recently, studies have provided evidence that the Gamma law well describes experimental data though they did not offer, contrary to our present study, the theory demonstrating the relevance of the law (Li et al., 2020; Verity et al., 2020). Using the θ-SEIHRD model to plan the need for beds, the study by Ivorra et al. (Ivorra,

Ferrández, Vela-Pérez, & Ramos, 2020) reported a PDF that systematically obeys the Gamma law, but again no theoretical demonstration was available. Finally, the SIDARTHE model, standing for Susceptible, Infected, Diagnosed, Ailing, Recognized, Threatened, Healed, and Extinct, introduced by Giordano et al. (Giordano et al., 2020) to predict the population contamination, also yielded skewed distributions of the Gamma type, in line with our approach.

COVID-19 has rapidly become a pandemic, and the fifth wave was still ongoing at the time of revision of the present article. Many countries worldwide have dealt with the situation, and the way they did it has varied. To date, there are few studies available classifying the impact of public health policies on COVID-19 cases or deaths. In our first study, we attempted to gather five countries where the approach has presumably been more rigorous at the early stage of the pandemic, according to the available literature (Bandyopadhyay & Meltzer, 2020; Laffet et al., 2021; Li, Lai, Gao, & Shi, 2021; Moshammer et al., 2020; Yom-Tov, 2021). In China, taken as the seminal country where the pandemic presumably started (Li et al., 2021), the observed data were not as smooth as expected due to the difficulty to count cases in a large country at an early stage. For instance, our attempt to correct the data by linearizing the curve to replace aberrant values and redistributing pro-rata extra-values in previous days failed to yield better theoretical fits than non-corrected data. As a result, we showed that our Gamma approach better fitted the observed data than did the Lognormal law in 5/5 countries (Study 1), the Gaussian law in 4/5 countries (except Israel), and the Weibull one in 3/5 countries (except Israel and New Zealand). New Gamma parameter $\bar{l}$ of 1.8 days in Study 1 was lower than that in Study 2 (3.7). We suggest that the new parameter $\bar{l}$ brings interesting new information. Within the five countries of Study 1, n was the lowest in China (17 against 19–38 for the other four countries). Parameter $\bar{l}$ was also lower than that of other countries (1.3 days against 1.3–3.1 elsewhere). The n variable representing the number of patients between the zero case and any case, a low value could mean that the national policy promptly controlled the situation, as suggested by Lai et al. (Lai et al., 2020). This value seems weak for China, given the country size and population density in cities where the pandemic started. Using GLEAM (Balcan et al., 2009), Chinazzi et al. (Chinazzi et al., 2020) predicted as early as January 2020 that the epidemic peak in China would occur by late April-early May if no action to reduce contamination would be taken. With the hindsight we now benefit from, the observed/Gamma peaks on February 8th/13th (i.e., 18–23 days after the epidemic start) indicate that the Chinese policy has been efficient in reversing the curve of daily cases (Lai et al., 2020). Our $\bar{l}$ value in days is reminiscent of the so-called serial interval (SI) of other studies though some specificities exist (Adam, 2020; He et al., 2020; Zhang et al., 2020). For He et al. (He et al., 2020), SI is the time of symptom onset between two successive cases in a contamination chain. In our approach, $\bar{l}$ stands for the time elapsed between the contamination of two successive cases, which is closer to the definition of SI by Adam et al. (Adam et al., 2020). The different description between He et al. (He et al., 2020) and our study is possibly sufficient to account for our $\bar{l}$ of 1.3 vs. their SI of 5.8 days in China (He et al., 2020) and 7.5 days on the *Diamond Princess* cruise ship (Zhang et al., 2020).

Our second study gathered the ten most impacted countries following our criteria (see Supplementary Material section S2). The policy has presumably been more tolerant at the early pandemic stage. The results showed that our Gamma approach better fitted the observed than did the Lognormal law in 10/10 countries (Study 2), the Gaussian law in 7/10 countries (except Spain, Slovenia, and Croatia), and the Weibull one in 7/10 countries (except Spain, Czechia, and Croatia). We saw above that the new Gamma parameter $\bar{l}$ was higher in Study 2 than in Study 1 (3.7 ± 1.4 against 1.8 ± 0.8 days, respectively). To clearly understand why a strict public health policy of detection-isolation decreases the parameter $\bar{l}$, there is a need to come back to the contamination tree (see Introduction section and Fig. 1). Let us imagine that a country policy allows restricting to 1 the number of contaminated patients by a given individual. The consequence is that patient P'_2 only contaminates patient P_3. Thus, the longest components l_3 ($P'_2P'_3$ and $P'_2P''_3$) are eliminated (see Fig. 1). The same occurs for successive patients (not shown in the figure) P_4, P_5, P_i ($3 < i \leq n$), thus reducing parameter $\bar{l}$. As Maier and Brockman (Maier & Brockmann, 2020) emphasized, each government strategy aiming at limiting the impact of the pandemic had a crucial role in the evolution of cases and deaths. This explains why the curve exhibited a sub-exponential start in China at the epidemic's beginning. In contrast, we expected a faster exponential starting curve, as was the case in H1N1 in 2009 (de Picoli Junior et al., 2011) or Ebola in 2014 (Hunt, 2014). Similarly, Flaxman et al. (Flaxman et al., 2020) have explored the critical role of non-pharmaceutical interventions in eleven European countries and shown that national lockdowns and closure of schools indeed reduced the spread of COVID-19. Consequently, any time delay in such interventions yields a PDF with a faster initial phase than expected by the Gamma law. For instance, this was the case in our study for Spain and Italy (see Fig. 3). Our demonstration and findings, together with the explanation of previous intuitive or qualitative studies (Giordano et al., 2020; Ivorra et al., 2020; Q. Li et al., 2020; Sanche et al., 2020; Verity et al., 2020), evidence that the temporal distribution of cases follows a Gamma law, which we defined here in extenso. Results also validate the general hypothesis according to which the distribution laws of all l_i are identical thus yielding Equation (3). More recently, Oliu-Barton et al. (Oliu-Barton et al., 2021) compared anti-COVID-19 measures of two groups of countries of the Organisation for Economic Co-operation and Development (OECD) depending on whether they chose a strategy of SARS-CoV-2 elimination or mitigation. In countries of their first group (gathering Australia, Island, Japan, New Zealand, and South Korea), the number of deaths was 25 times weaker than that of countries of their second group (Austria, Belgium, Canada, Chile, Colombia, Czechia, Denmark, Estonia, Finland, France, Germany, Greece, Hungary, Ireland, Israel, Italy, Latvia, Lithuania, Luxembourg, Mexico, Netherlands, Norway, Poland, Portugal, Slovakia, Slovenia, Spain, Sweden, Switzerland, Turkey, the UK, and the USA). Though their study did not mention the SI, we reexamined our data using their classification and our selection criteria (see Supplementary Material section S2). Only one country (New Zealand) remained in our first group, while ten countries made up the second group (Austria, Belgium, Czechia, Finland, France, Germany, Israel, Italy, Slovenia, Spain). Consistent with our initial classification, our Gamma $\bar{l}$ value was 1.3 days in only New Zealand vs. 3.1 days in the new group of 10 countries. In other words, an elimination strategy of

SARS-CoV-2 may yield a lower $\bar{l}$ than does a mitigation strategy. The influence of public health policy on parameter n is more challenging to demonstrate. Only a stringent policy may limit the number of cascades in the contamination chain and finally stop the epidemic. This is what we observe in China, a large and high populated country, where the number of cascades might be potentially enormous if one waits the pandemic to vanish itself. However, parameter n is only 17 in China, the lowest of our first group, probably due to the rigorous policy of isolation (complete lockdown). In our Study 2, low values of n could be observed, which always concerned small and low populated countries where the patient reservoir is limited. Our assumption is corroborated by the observation that the pandemic can end when the availability of susceptible individuals decreases (Cobey, 2020). In summary, we suggest that parameters n and $\bar{l}$ are influenced by each country's national public health policy, though differently. Parameter $\bar{l}$ is lowered as soon as the country takes efficient measures of detection-isolation, whereas parameter n may only be influenced by a full and rigid lockdown.

To conclude, as COVID-19 spread draws a contamination tree, it is virtually possible to apply our Gamma law approach to any problem involving a branching system. Nature offers many branching systems: rivers, trees and plants, aerial branching system, underground roots, corals and lichens, phylogenetic trees in genetics, family tree structure in demography, dendritic growth of crystals. Further applications may concern biology and physiology: blood networks, lung networks, neural networks, etc. Thus, our Gamma law approach offers promising directions to inspire future scientists in various disciplines involving branching systems.

Author contributions

JD and OAC conceived the study and wrote the manuscript.
JD developed the mathematical theory and algorithm.
OAC made the coding.

Data availability statement

Data are fully and freely available at https://www.worldometers.info/coronavirus/.

Declaration of competing interest

The authors declare no conflict of interest.

Acknowledgments

None.

Appendix A. Supplementary data

Supplementary data to this article can be found online at https://doi.org/10.1016/j.idm.2022.02.004.

References

Adam, D. (2020). Special report: The simulations driving the world's response to COVID-19. *Nature, 580*(7803), 316–318. https://doi.org/10.1038/d41586-020-01003-6

Adam, D. C., Wu, P., Wong, J. Y., Lau, E. H. Y., Tsang, T. K., Cauchemez, S., … Cowling, B. J. (2020). Clustering and superspreading potential of SARS-CoV-2 infections in Hong Kong. *Nature Medicine, 26*(11), 1714–1719. https://doi.org/10.1038/s41591-020-1092-0

Anderson, R. M., Fraser, C., Ghani, A. C., Donnelly, C. A., Riley, S., Ferguson, N. M., … Hedley, A. J. (2004). Epidemiology, transmission dynamics and control of SARS: The 2002-2003 epidemic. *Philosophical Transactions of the Royal Society of London Series B Biological Sciences, 359*(1447), 1091–1105. https://doi.org/10.1098/rstb.2004.1490

Anderson, R. M., & May, R. M. (1991). *Infectious diseases of humans: Dynamics and control*. Oxford, UK: Oxford University Press.

Balcan, D., Colizza, V., Gonçalves, B., Hu, H., Ramasco, J. J., & Vespignani, A. (2009). Multiscale mobility networks and the spatial spreading of infectious diseases. *Proceedings of the National Academy of Sciences of the United States of America, 106*(51), 21484–21489. https://doi.org/10.1073/pnas.0906910106

Bandyopadhyay, G., & Meltzer, A. (2020). Let us unite against COVID-19 - a New Zealand perspective. *Irish Journal of Psychological Medicine, 37*(3), 218–221. https://doi.org/10.1017/ipm.2020.44

Cauchemez, S., Bhattarai, A., Marchbanks, T. L., Fagan, R. P., Ostroff, S., Ferguson, N. M., et al. (2011). Role of social networks in shaping disease transmission during a community outbreak of 2009 H1N1 pandemic influenza. *Proceedings of the National Academy of Sciences of the United States of America, 108*(7), 2825–2830. https://doi.org/10.1073/pnas.1008895108

Chinazzi, M., Davis, J. T., Ajelli, M., Gioannini, C., Litvinova, M., Merler, S., … Vespignani, A. (2020). The effect of travel restrictions on the spread of the 2019 novel coronavirus (COVID-19) outbreak. *Science, 368*(6489), 395–400. https://doi.org/10.1126/science.aba9757

Cho, H. K., Bowman, K. P., & North, G. R. (2004). A comparison of Gamma and lognormal distributions for characterizing satellite rain rates from the Tropical Rainfall Measuring Mission. *Journal of Applied Meteorology and Climatology, 43*(11), 1586–1597.

Cobey, S. (2020). Modeling infectious disease dynamics. *Science, 368*(6492), 713–714. https://doi.org/10.1126/science.abb5659

Collett, D. (2015). *Modelling survival data in medical research* (3rd ed.). New York: Chapman and Hall/CRC.

Faye, O., Boëlle, P. Y., Heleze, E., Faye, O., Loucoubar, C., Magassouba, N., … Cauchemez, S. (2015). Chains of transmission and control of Ebola virus disease in Conakry, Guinea, in 2014: An observational study. *The Lancet Infectious Diseases, 15*(3), 320–326. https://doi.org/10.1016/s1473-3099(14)71075-8

Ferguson, N. M., Cummings, D. A., Cauchemez, S., Fraser, C., Riley, S., Meeyai, A., … Burke, D. S. (2005). Strategies for containing an emerging influenza pandemic in Southeast Asia. *Nature, 437*(7056), 209–214. https://doi.org/10.1038/nature04017

Ferguson, N. M., Cummings, D. A., Fraser, C., Cajka, J. C., Cooley, P. C., & Burke, D. S. (2006). Strategies for mitigating an influenza pandemic. *Nature, 442*(7101), 448–452. https://doi.org/10.1038/nature04795
Flaxman, S., Mishra, S., Gandy, A., Unwin, H. J. T., Mellan, T. A., Coupland, H., … Bhatt, S. (2020). Estimating the effects of non-pharmaceutical interventions on COVID-19 in Europe. *Nature*. https://doi.org/10.1038/s41586-020-2405-7
Giordano, G., Blanchini, F., Bruno, R., Colaneri, P., Di Filippo, A., Di Matteo, A., et al. (2020). Modelling the COVID-19 epidemic and implementation of population-wide interventions in Italy. *Nature Medicine, 26*(6), 855–860. https://doi.org/10.1038/s41591-020-0883-7
Graw, F., & Perelson, A. S. (2016). Modeling viral spread. *Annual Review of Virology, 3*(1), 555–572. https://doi.org/10.1146/annurev-virology-110615-042249
He, X., Lau, E. H. Y., Wu, P., Deng, X., Wang, J., Hao, X., … Leung, G. M. (2020). Temporal dynamics in viral shedding and transmissibility of COVID-19. *Nature Medicine, 26*(5), 672–675. https://doi.org/10.1038/s41591-020-0869-5
Hunt, A. G. (2014). Exponential growth in Ebola outbreak since may 14, 2014. *Complexity, 20*(2), 8–11.
Ivorra, B., Ferrández, M. R., Vela-Pérez, M., & Ramos, A. M. (2020). Mathematical modeling of the spread of the coronavirus disease 2019 (COVID-19) taking into account the undetected infections. The case of China. *Communications in Nonlinear Science and Numerical Simulation, 88*, 105303. https://doi.org/10.1016/j.cnsns.2020.105303
Laffet, K., Haboubi, F., Elkadri, N., Georges Nohra, R., & Rothan-Tondeur, M. (2021). The early stage of the COVID-19 outbreak in Tunisia, France, and Germany: A systematic mapping review of the different national strategies. *International Journal of Environmental Research and Public Health, 18*(16). https://doi.org/10.3390/ijerph18168622
Lai, S., Ruktanonchai, N. W., Zhou, L., Prosper, O., Luo, W., Floyd, J. R., … Tatem, A. J. (2020). Effect of non-pharmaceutical interventions to contain COVID-19 in China. *Nature*. https://doi.org/10.1038/s41586-020-2293-x
Lancaster, H. O. (1966). Forerunners of the pearson chi-square. *Australian Journal of Statistics, 8*, 117–126.
Laplace, P. S. (1836). *Théorie analytique des probabilités, suppl. to 3rd edn*. Paris: Courcier.
Li, Q., Guan, X., Wu, P., Wang, X., Zhou, L., Tong, Y., … Feng, Z. (2020). Early transmission dynamics in Wuhan, China, of novel coronavirus-infected pneumonia. *New England Journal of Medicine, 382*(13), 1199–1207. https://doi.org/10.1056/NEJMoa2001316
Li, J., Lai, S., Gao, G. F., & Shi, W. (2021). The emergence, genomic diversity and global spread of SARS-CoV-2. *Nature, 600*(7889), 408–418. https://doi.org/10.1038/s41586-021-04188-6
Lin, Q., Zhao, S., Gao, D., Lou, Y., Yang, S., Musa, S. S., … He, D. (2020). A conceptual model for the coronavirus disease 2019 (COVID-19) outbreak in Wuhan, China with individual reaction and governmental action. *International Journal of Infectious Diseases, 93*, 211–216. https://doi.org/10.1016/j.ijid.2020.02.058
Maier, B. F., & Brockmann, D. (2020). Effective containment explains subexponential growth in recent confirmed COVID-19 cases in China. *Science, 368*(6492), 742–746. https://doi.org/10.1126/science.abb4557
Massey, Jr., F. J. (2012). The Kolmogorov-Smirnov test for goodness of fit. *Journal of the American Statistical Association, 46*(253), 68–78.
Moshammer, H., Poteser, M., Lemmerer, K., Wallner, P., & Hutter, H. P. (2020). Time course of COVID-19 cases in Austria. *International Journal of Environmental Research and Public Health, 17*(9). https://doi.org/10.3390/ijerph17093270
Neuberger, A., Paul, M., Nizar, A., & Raoult, D. (2013). Modelling in infectious diseases: Between haphazard and hazard. *Clinical Microbiology and Infections, 19*(11), 993–998. https://doi.org/10.1111/1469-0691.12309
Oliu-Barton, M., Pradelski, B. S. R., Aghion, P., Artus, P., Kickbusch, I., Lazarus, J. V., … Vanderslott, S. (2021). SARS-CoV-2 elimination, not mitigation, creates best outcomes for health, the economy, and civil liberties. *Lancet, 397*(10291), 2234–2236. https://doi.org/10.1016/s0140-6736(21)00978-8
de Picoli Junior, S., Teixeira, J. J., Ribeiro, H. V., Malacarne, L. C., dos Santos, R. P., & dos Santos Mendes, R. (2011). Spreading patterns of the influenza A (H1N1) pandemic. *PLoS One, 6*(3), Article e17823. https://doi.org/10.1371/journal.pone.0017823
Sanche, S., Lin, Y. T., Xu, C., Romero-Severson, E., Hengartner, N., & Ke, R. (2020). High contagiousness and rapid spread of severe acute respiratory syndrome coronavirus 2. *Emerging Infectious Diseases, 26*(7). https://doi.org/10.3201/eid2607.200282
Thompson, R. N., Hollingsworth, T. D., Isham, V., Arribas-Bel, D., Ashby, B., Britton, T., & Restif, O. (2020). Key questions for modelling COVID-19 exit strategies. *Proceedings: Biological sciences, The Royal Society, 287*(1932), 20201405. https://doi.org/10.1098/rspb.2020.1405
Verity, R., Okell, L. C., Dorigatti, I., Winskill, P., Whittaker, C., Imai, N., … Ferguson, N. M. (2020). Estimates of the severity of coronavirus disease 2019: A model-based analysis. *The Lancet Infectious Diseases, 20*(6), 669–677. https://doi.org/10.1016/s1473-3099(20)30243-7
Woo, G. (1999). *The mathematics of natural catastrophes*. London, UK: Imperial College Press.
Yom-Tov, E. (2021). Active syndromic surveillance of COVID-19 in Israel. *Scientific Reports, 11*(1), 24449. https://doi.org/10.1038/s41598-021-03977-3
Zhang, S., Diao, M., Yu, W., Pei, L., Lin, Z., & Chen, D. (2020). Estimation of the reproductive number of novel coronavirus (COVID-19) and the probable outbreak size on the Diamond princess cruise ship: A data-driven analysis. *International Journal of Infectious Diseases, 93*, 201–204. https://doi.org/10.1016/j.ijid.2020.02.033